npj | clean water

www.nature.com/npjcleanwater

ARTICLE OPEN

Check for updates

Electrohydrodynamic atomization of CNT on PTFE membrane for scaling resistant membranes in membrane distillation

Lijo Francis[1] and Nidal Hilal[1]✉

In this study, an electrohydrodynamic atomization or electrospraying technique is used for the uniform deposition of carbon nanotubes (CNT) on a commercially available PTFE membrane and employed for Membrane Distillation (MD) process. Modified PTFE-CNT membrane was characterized for water contact angle, liquid entry pressure (LEP), pore size distribution, and surface morphology. The electrospray coating of CNT on the PTFE membrane enhances the turbulence and thereby the temperature polarization coefficient (TPC). The pore size of the micropatterned PTFE-CNT membrane has been reduced and pore size distribution has been narrowed compared to the PTFE membrane. Field-effect scanning electron microscopy images of the membranes were observed before and after the MD process. Functionally graded PTFE-CNT membrane showed superior desalination performance compared to the PTFE membrane with less amount of cake layer formation on the membrane surface. Water vapor flux remained constant during 24-h continuous MD process operation with 99.99% rejection of inorganic salts.

npj Clean Water (2023)6:15 ; https://doi.org/10.1038/s41545-023-00229-x

INTRODUCTION

Functionally graded nanostructured membranes have recently gained researchers' attention as they enhance the parent membrane properties and stimulate the process performance. The efflorescing membrane-based water treatment processes include membrane distillation (MD, forward osmosis (FO), pressure retarded osmosis (PRO), reverse electrodialysis (RED), and/or their hybrids for the respective niches. Seawater reverse osmosis (SWRO) is a matured and conventional membrane-based seawater desalination technology. Possible efforts to improve the specific energy consumption (SEC) and production cost along with the greening of desalination processes are significantly in progress with the aid of nanostructured membranes and engineered processes[1–6]. Thermally-driven conventional seawater desalination processes are multi-stage flash (MSF) and multi-effect distillation (MED) and, they are considered matured technologies. SWRO and emerging membrane-based desalination technologies are considered superior to conventional thermal desalination technologies due to their considerably low energy consumption and total water production cost. The renewable energy-driven sustainable desalination process is gaining much attention because of the increasing water scarcity and global climate change due to deteriorating environmental scenarios such as deforestation, weather change, and increasing pollution. Solar energy, geothermal energy, wind energy, and ocean thermocline are some of the renewable energies that can be utilized for generating power to operate the industrial desalination processes. Effective use of renewable energy sources helps to minimize the usage of fossil fuel energy and thereby the greenhouse gas (GHG) emissions[7–10].

Researchers have used many methods such as membrane engineering, advanced module engineering, and process engineering to enhance water treatment performance[11–14]. Electrohydrodynamic atomization (EHDA) is also known as electrospraying in which a solution or a dispersion flowing from a capillary nozzle is subjected to a strong electric field by applying a high electric potential. Vatanpour et al. highlighted a review article on the fabrication of different types of polymeric and ceramic separation membranes using the electrospraying technique and employed them for different applications. They have also highlighted the current challenges and opportunities of electrospraying in membrane fabrication[15,16]. Functionally graded nanocomposite membranes can be efficiently engineered and have been used for water treatment applications as they have versatile characteristics[17–22]. They are fabricated either by the modification of commercially available membranes or by the direct fabrication of the functionalized membranes from their respective precursors. In one of our previous studies, hydroxyapatite (HA) nanoparticles were deposited on an electrospun gelatin substrate via electrospraying and successfully tested for bone tissue regeneration[23]. In another study, a nanocomposite polyimide membrane with enhanced membrane characteristics was fabricated by simultaneous electrospinning and electrospraying of titania nanoparticles[24]. Jia et al., have demonstrated the fabrication of a superhydrophilic/superhydrophobic layer on a PVDF substrate via sequential electrospraying technique and used for the MD process. Octaphenylsilsesquioxane (POSS) nanoparticles were deposited on polyvinylidene fluoride (PVDF) substrate via electrospraying to create a superhydrophobic layer with multiscale roughness. They have also reported that the membranes have anti-wetting and antifouling properties[25]. Shahabadi et al., fabricated a nanostructured membrane with polyvinylidene fluoride-co-hexafluoropropylene (PVDF-CFP) and functionalized titania nanoparticles via electrospinning and electrospraying, and used it for the MD process. They reported that the modified membrane was superhydrophobic and showed superior water permeation flux compared to the commercial membrane[26]. Attia et al. used electrospinning and electrospraying techniques for the fabrication of a robust MD membrane with enhanced performance. They used PVDF and alumina nanoparticles for electrospinning and electrospraying, respectively[27]. Su et al. reported the

[1]NYUAD Water Research Center, New York University Abu Dhabi, Abu Dhabi, P.O. Box 129188, United Arab Emirates. ✉email: nidal.hilal@nyu.edu

fabrication of a robust PVDF-CFP electrospun membrane along with the electrospraying of silica nanoparticles. The fabricated MD membranes were superhydrophobic with excellent scaling resistance[28]. On the other hand, Hong et al. reported a pore-size tunable superhydrophobic membrane for the MD process. A blend of polydimethylsiloxane (PDMS)/PVDF-CFP was used for electrospraying on an electrospun polyurethane membrane and observed enhanced desalination performance. The results were studied by modeling tools and observed matching correlations[29].

In the current study, an electrohydrodynamic atomization (EHDA) or electrospraying technique is used to deposit a uniform coating of carbon nanotubes (CNT) on a commercially available PTFE membrane and employed for Membrane Distillation (MD) process. PTFE-CNT membranes showed superior MD membrane characteristics and process performance compared to the PTFE membrane during 24-h DCMD operation. Micropatterned CNTs deposited on the PTFE membrane yield increased temperature polarization coefficient (TPC) and thereby superior process performance. Scanning electron microscopy (SEM) of PTFE-CNT membranes, before and after the MD process reveals that the salt deposition or scaling propensity is significantly less than that of PTFE membranes. Thus, electrospraying of CNT or suitable nanomaterials on MD membranes can be considered a robust method for fabricating durable membranes with anti-scaling, less pore wetting, and enhanced MD performance.

RESULTS AND DISCUSSION

MD membrane characteristics

All the results discussed in this section are formulated from the average of three consecutive experiments. Selection of appropriate membrane/materials and suitable nanomaterials with the proper aid of uniform coating technique is the key to improve the membrane characteristics. Electrohydrodynamic atomization of CNTs or any other nanomaterial dispersion provides a very uniform coating on the base membrane surface and improve the membrane efficiency. High water contact angle (>120°), optimum pore size (0.2 µm), high porosity (>75%) and narrow pore size distribution are recommended for an efficient MD membrane. In a recent report Mustafa et al. demonstrated the influence of super hydrophobic carbon nanomaterial coating on PVDF-CFP membrane to improve the membrane characteristics and desalination performance. Water contact angle increased from 83° to 124° and porosity of the membrane increased from 45.3% to 86.9%. The highest reported flux in this study was 77 LMH at a high feed solution temperature of 85 °C[30].

Table 1. Water contact angle and pore size distribution data of PTFE and PTFE-CNT membranes.

Membrane	PTFE	PTFE-CNT
Water contact angle	130 ± 2°	136 ± 3°
Minimum pore size (µm)	0.0430	0.0353
Mean Flow Pore Size (µm)	0.1562	0.1489
Pore size at the bubble point or maximum pore size (µm)	0.36	0.292
Bubble point pressure (PSI)	18.329	22.579

Water contact angle and pore size distribution

1H,1H, 2H, 2H- perfluorooctyl triethoxy silane was used as the binder while doing electrospraying of CNT on the PTFE membrane. It is not only a binder but also a dispersant and highly hydrophobic reagent. The observed water contact angle of the PTFE-CNT membrane is higher than the pristine PTFE membrane. Modified CNT would enhance the surface roughness and thereby increase the water contact angle. The increase in the average water contact angle is calculated to be 4.6%. Water contact angle, mean flow pore size, minimum pore size, bubble point, and corresponding pressure of the PTFE and PTFE-CNT membranes are tabulated in Table 1. Servi et al. conducted a scientific study of the effect of hydrophobicity on the MD membrane wetting. They reported that the LEP increases with the water contact angle and which enhances the MD process performance[31].

Percentage pore size distribution of PTFE and PTFE-CNT electrosprayed membranes are shown in Fig. 1. It is evident from Fig. 1 and Table 1 that the electrosprayed CNT particles are the cause of pore size reduction and more narrow pore size distribution. Shahabadi et al., have reported that narrow pore size distribution is better for enhanced MD performance[26]. The reduction in minimum pore size, mean flow pore size, and maximum pore sizes are calculated as 17.9%, 4.7%, and 18.9 %, respectively.

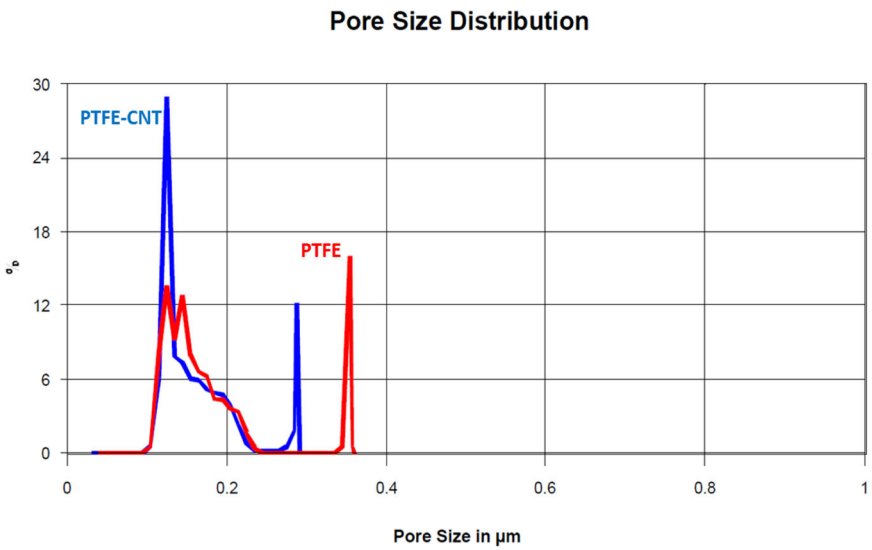

Fig. 1 Percentage pore size distribution of PTFE and PTFE-CNT membranes.

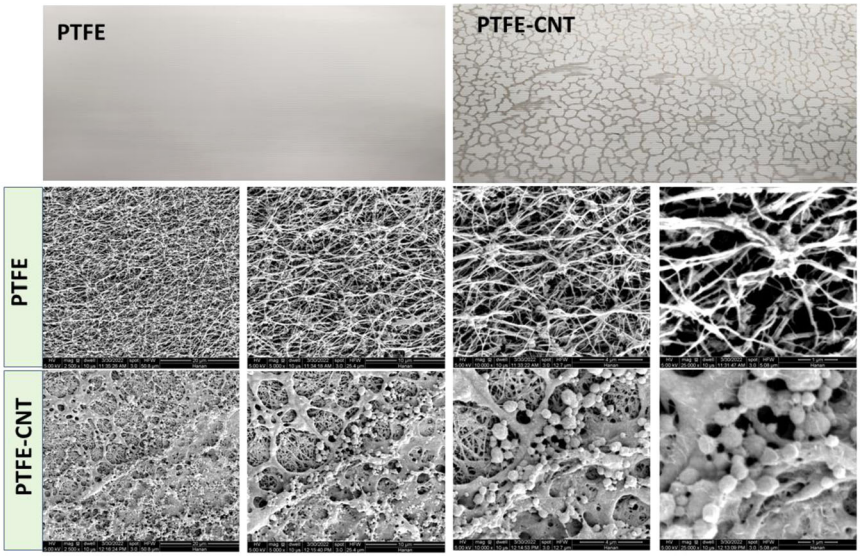

Fig. 2 Photo snaps and SEM Images of PTFE membrane and electrosprayed PTFE-CNT membrane at different magnifications.

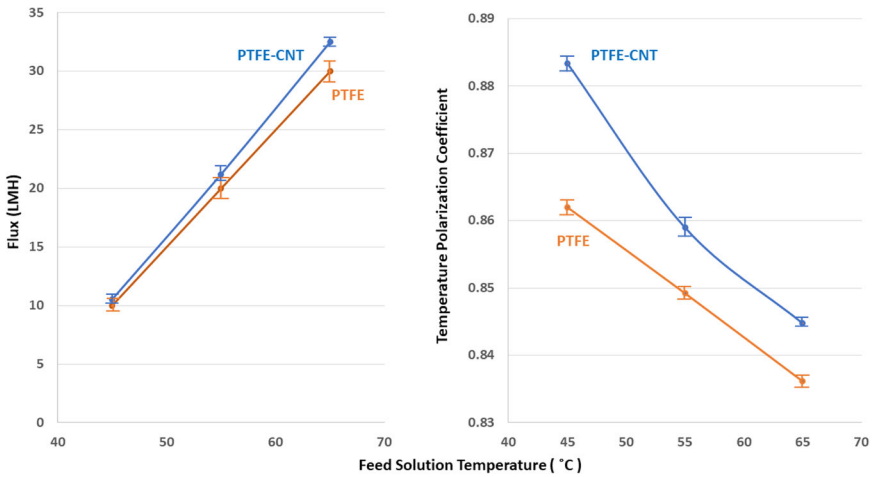

Fig. 3 Water permeate flux and TPC values during a 24-h DCMD test using PTFE and PTFE-CNT membranes at a constant coolant temperature of 15 °C.

Liquid entry pressure

A reduction in the pore size may lead to an increased LEP value for the PTFE-CNT electrosprayed membrane compared to the PTFE membrane. Similar results are also reported by Calaramunt et al.[32]. As expected, the CNT-doped PTFE membranes have a higher LEP value than PTFE membranes. Reduced pore size and increased water contact angle result in the increased average LEP. Pore wetting is a great concern in processes such as MD and the highest possible LEP is a very important parameter to mitigate the pore wetting phenomenon. PTFE-CNT membrane showed a 4.1% increase in the LEP value (4.83 bar) than that of a non-modified PTFE membrane (4.64 bar). In the long run, increased water contact angle, reduced pore size, narrow pore size distribution, and increased LEP would reduce the membrane fouling and pore wetting phenomenon, and increase the membrane shelf life. Thereby, membrane cleaning frequency can be extended, and less amount of chemicals would be needed for membrane cleaning. Zhang et al. studied the effect of hydrophobicity on membrane fouling and wetting. They reported that highly hydrophobic surfaces are better to reduce the interaction between membrane surface and feed solution and, reduce the membrane fouling and wetting[33].

Surface morphology

Figure 2 shows photo snaps and FESEM images of the PTFE membrane and electrosprayed PTFE-CNT membrane. Knot-fibril structured porous morphology is evident from the SEM images of the PTFE membrane.

CNT particles are uniformly distributed throughout the membrane surface is also evident from the SEM images and the photo image. CNT particles or their clusters are restricting some of the PTFE membrane pores is the reason for reducing the membrane pore size and narrowing the pore size distribution as shown in Fig. 1. Thus, the electrospraying method helps to create micropatterns of CNTs on the hydrophobic PTFE membrane. Doped nanoparticles would enhance the surface roughness and water contact angle. This is the reason for increasing the LEP values and decreasing the pore sizes of PTFE-CNT membranes more than that of PTFE membranes.

DCMD experiments

Water permeate flux during a 24-h DCMD test using a PTFE membrane with time at different ΔT has been calculated. Data login has been initiated after stabilizing the temperature on the feed and permeate side. Feed solution temperature was ramped

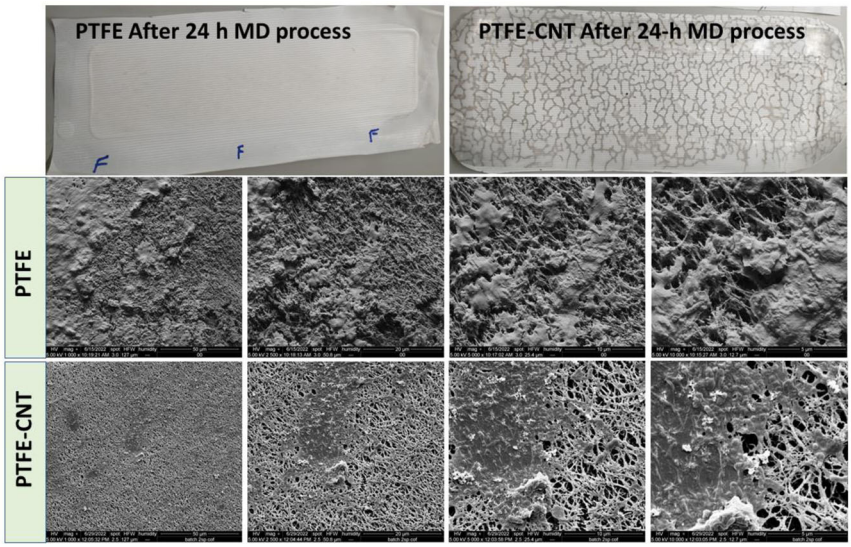

Fig. 4 Photo images and FESEM images of PTFE and PTFE-CNT membranes after 24-h DCMD operation.

from 45 °C to 55 °C and then to 65 °C. Data has not been logged during ramping and stabilizing of the temperatures on the feed and coolant sides. Each time ΔT kept constant for 8 h. It is evident from calculated data that there is no flux decay during 24-h continuous MD operation. About 50% of freshwater was recovered from the feed and the concentration of feed solution increased from 1% to 2% with nearly 100% salt rejection. It is well known that the MD process can theoretically reject 100% inorganic salts and MD can operate at significantly very high salt concentrations. Therefore, the MD process is recommended for recovering fresh water from thermal and SWRO brines.

Figure 3 shows the water permeate flux and calculated TPC values during the DCMD tests using PTFE and PTFE-CNT membranes at various feed solution temperatures and constant coolant temperature (15 °C). Trans-membrane vapor pressure increases as ΔT increases across the membrane. Eventually, water permeate flux increases as is evident from Fig. 3. While using the PTFE membrane, permeate flux was found to be increased from 10 LMH to 20 LMH and then to 30 LMH, when ΔT increased from 30 °C to 40 °C and then to 50 °C, respectively. A similar trend was observed while using the PTFE-CNT membrane. Permeate flux was found to be increased from 5%, 6%, and 8.3% while using the PTFE-CNT membrane compared to the PTFE membrane, when ΔT was increased from 30 °C to 40 °C, and then to 50 °C, respectively.

TPC values are calculated from the registered temperatures of feed and coolant solutions before entering and after exiting from the membrane module, during the DCMD operation. TPC is a measure of the TP phenomenon. An efficient MD process should have the highest possible TPC value. The theoretical maximum of the TPC value is 1. The thickness of the polarization layer adjacent to the MD membrane decreases with the increase in TPC value[34,35]. Turbulence-promoting methods such as employing the spacers, flashing the feed, engineered bubbling, etc. could reduce the polarization boundary layer towards the membrane surface, and the subsequent increase in TPC values. In the current study, the highest TPC value calculated is 0.88 while using PTFE-CNT membrane at feed and coolant solution temperatures of 45 °C and 15 °C, respectively. Thus a 2.5% increase in TPC value was observed while using electrosprayed PTFE-CNT membrane compared to PTFE membrane. Electrospraying of CNTs would create micropatterns of CNTs on the PTFE membrane surface. As it is evident from the aforementioned membrane characterizations, micropatterned CNT would generate some microturbulence to the feed solution near the membrane surface and cause a reduction in the thickness of the polarization layer. While increasing the feed solution temperature, trans-membrane vapor pressure increases and leads to faster permeate evaporation. An increase in heat and mass transfer leads to an increase in the thickness of the polarization layer. This is the reason for decreasing TPC values while increasing feed temperature.

Figure 4 shows the photo images and FESEM images of PTFE and PTFE-CNT membranes after 24-h DCMD operation. CNT micropatterns are visibly intact on the PTFE membrane even after a 24-h process test. Surface morphology observed at different locations in the membrane samples reveals that salt deposition is much lower on the PTFE-CNT membrane than that on the PTFE membrane. Electrosprayed CNT particles could reduce the scaling and cake-layer formation on the membrane surface during the desalination process. CNT micropatterns could create a micro-turbulence that could be attributed to the reduced salt deposition on the membrane surface. This will enhance the membrane life and reduce the volume of chemicals required for membrane cleaning. With the aid of advanced technologies, large-scale electrohydrodynamic atomization is possible[36–38]. Hence, the modified PTFE membranes with CNT nanoparticles could contribute to the enhanced process performance with reduced membrane scaling and pore wetting and, a reduction in the GHG emissions.

In conclusion, electrospraying is an efficient technique for depositing CNTs and other nanostructured materials on membrane surfaces. Membrane properties can be efficiently engineered through electrospray deposition as per the requirement. The water contact angle is increased on a modified CNT electrosprayed PTFE membrane. The average pore size, and minimum and maximum pore sizes of the PTFE-CNT membrane have been reduced compared to the pristine PTFE membrane. The pore size distribution of the modified CNT-PTFE membrane has been narrowed than the nascent PTFE membrane. Increased water contact angle and reduced pore sizes lead to the increased LEP which is a favorable MD membrane characteristic as it helps to reduce the pore wetting phenomenon. FESEM images reveal the presence of CNTs on the modified PTFE membrane. DCMD water permeate flux while using the PTFE-CNT membrane was observed as high as 8.3% compared to the PTFE membrane. The calculated TPC value during DCMD operation when using the CNT electrosprayed PTFE membrane was calculated as high as 2.5% compared to the PTFE membrane. Increased TPC value reduces the TP phenomenon by reducing the thickness of the polarization

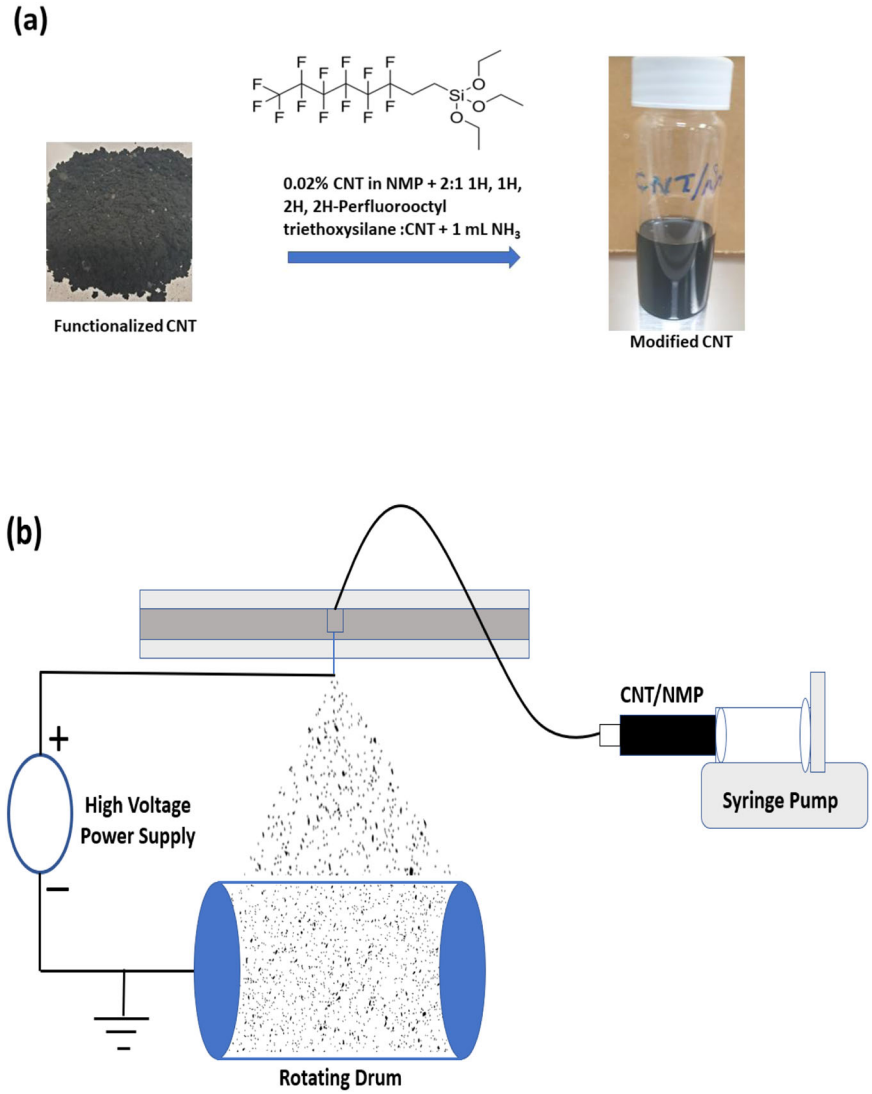

Fig. 5 Electrospraying process. a Preparation of modified CNT/NMP dispersion, and **b** Electrospraying of CNT/NMP dispersion.

layer adjacent to the membrane surface. No flux decay was observed during the 24-h operation and the feed solution was concentrated from 1% to 2% during the MD process with >99.99% salt rejection. CNTs have very strongly adhered to the membrane surface as the CNT micropatterns are visible on the membrane surface even after a 24-h continuous MD test. Moreover, the salt deposition on the PTFE-CNT membrane is much lower than that on the PTFE membrane. This would enhance the membrane shelf life and chemicals required for cleaning during the desalination process in a long run. Electrospray deposition forms CNT micropatterns on the PTFE membrane, which creates microturbulence in the feed solution adjacent to the membrane surface. It leads to an increased TPC value and reduced salt deposition propensity during the DCMD operation.

METHODS

Materials

PVDF, PTFE and poly propylene (PP) are the most commonly used polymeric materials used for MD membrane fabrication. Among these, PTFE is most suitable material due to its high hydrophobicity, low surface energy, high chemical stability, low intermolecular attraction and high crystallinity[39,40]. Commercially available polypropylene scrim-backed polytetrafluoroethylene (PTFE) membrane was purchased from Sterlitech Corporation, USA. Functionalized multiwall carbon nanotubes (MWCNT), N-methyl pyrrolidone (NMP), and 1H,1H, 2H, 2H- perfluorooctyl-triethoxysilane (POTS) were purchased from Sigma Aldrich.

Electrospraying of CNT

Hydrophobically modified perfluorinated CNTs were prepared as per the procedure followed by Georgakilas et al.[41]. POTS was used as a dispersant and binder for CNTs. A schematic representation of the preparation of modified CNT-NMP dispersion and electrospraying of CNT-NMP dispersion are shown in Fig. 5a, b, respectively. The modified CNT-NMP dispersion was taken in a syringe and subjected to electrospraying using a Mecc Nanon Electrospinning setup purchased from Japan. The dispersion taken in the syringe was mounted on a syringe pump which drives the dispersion through a plastic tube to the 18 G-sized blunted syringe needle mounted 10 cm above the rotating drum. From-side-to-side movement of the syringe needle along the rotating drum and speed of the rotating drum can be controlled. PTFE membrane was mounted on the rotating drum before the electrospraying. Variable parameters used for electrospraying are the concentration of the dispersion, flow rate, applied voltage, distance between the syringe needle tip and grounded rotating drum, speed of the rotating drum, and speed of

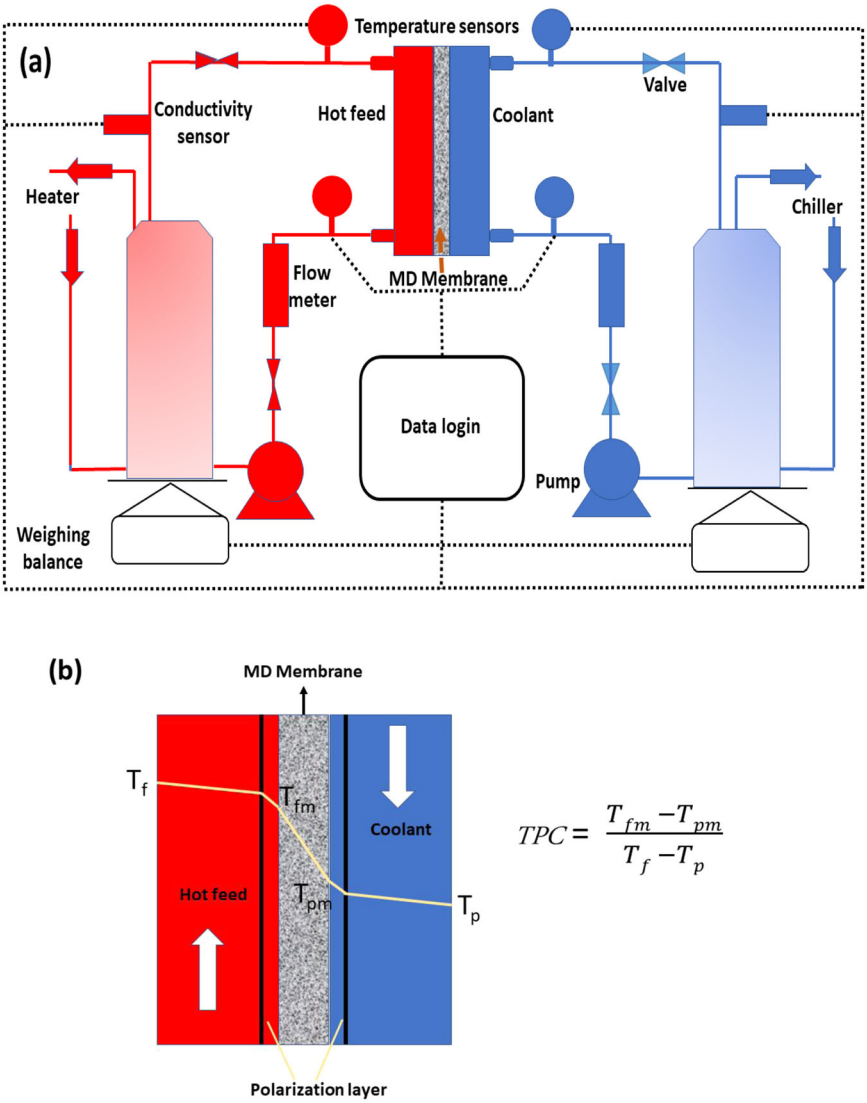

Fig. 6 Direct contact membrane distillation (DCMD) process. a Schematic representation of experimental DCMD setup, and **b** the TP profile in a DCMD process.

the syringe needle along the rotating drum. The positive terminal of the high voltage power supply was connected to the syringe needle and the negative terminal was connected to the grounded rotating drum. 10 mL of CNT-NMP dispersion was electrosprayed on the PTFE membrane at a flow rate of 1 mL/h by applying an electric voltage of 20 kV. The speed of the rotating drum and syringe needle movement was set at 100 rpm and 5 mm/s, respectively to obtain a uniform CNT coating on the PTFE membrane surface.

Water contact angle measurements

The water contact angle of PTFE and PTFE-CNT membranes was measured using a drop shape analyzer -DSA 100 purchased from Kruss Scientific, Germany. Three pieces of PTFE and PTFE-CNT membrane samples were used for the measurements. Water contact angles at five different locations in each membrane sample were measured and the average value is considered as the water contact angle of respective membranes.

Mean pore size, bubble point, and pore size distribution

An advanced capillary flow porometer purchased from Porous Materials Inc, USA (iPore-1500A) was used for bubble point, mean flow pore size, and pore size distribution analysis of PTFE and CNT coated PTFE membranes. Circular membrane samples with 25 mm diameter were used for the analysis. This equipment is based on capillary flow porometry, where a nontoxic wetting liquid is allowed to spontaneously fill the membrane pores and a non-reacting gas (Nitrogen) is allowed to displace liquid from pores. In the current study, a Galwick fluid having a very low surface tension of 15.9 dynes/cm was used to wet the hydrophobic membrane before the pore size analysis. When Nitrogen gas inserts pressure on the membrane gradually, the largest pores will get emptied first, as they need lower pressure than smaller pores. High pressure is required to empty the Galwick fluid from small pores. The pressure and flow rate of gas through the emptied pores provide the through pore distribution. The pressure at which pores are empty is inversely proportional to the pore size. An average of three sample measurements are given in Table 1.

Liquid entry pressure (LEP) test

LEP is an important parameter in water treatment processes where the membrane has to stay non-wetted[42]. LEP test was carried out using an automated LEP analyzing Convergence Minos system purchased from the Convergence Industry, Netherlands.

The LEP of the tested membrane is determined by applying small pressure increment steps. After each step, the pressure decay is measured. If no wetting of the membrane takes place, the pressure decay will be zero. When wetting starts to occur, a pressure decay is observed and the test is stopped. The system allows the pressure ramp to be configured, and the system automatically flushes before the start of the experiment to remove air bubbles. Circular membrane samples with 25 mm diameter were used for the LEP measurements at a step size of 0.1 bar in this study. An average LEP value of 3 membrane samples was calculated.

Surface morphology

Surface morphology of PTFE and CNT coated PTFE membranes, before and after MD experiments was observed using Thermo Fischer Field-Effect Scanning Electron Microscope (FESEM) Quanta 450, USA. Membrane samples were sputter-coated using a Gold plate, before the SEM imaging.

Temperature polarization coefficient (TPC)

Temperature polarization (TP) occurs only in non-isothermal processes such as MD and as a result the driving force -trans-membrane vapor pressure difference decreases[43,44]. As a thermally-driven membrane-based process, one of the major limitations associated with MD is the TP phenomenon. Heat and mass transfer are combined in all thermal-based separation processes[45,46]. The TP is experienced in the thin layer of the liquid stream adjacent to the membrane surface during the heat and mass transfer process in an MD operation. TP reduces the trans-membrane vapor pressure difference and it is also contributing to the fouling and scaling phenomenon on the membrane surfaces. Many studies have been carried out to mitigate the TP phenomenon. Employing spacers, baffles, etching on the membranes, engineered bubbling, stirring, flashing the feed, and employing isolation barriers are some methods adapted for mitigating the TP[47–53]. TPC is a measure of the TP phenomenon. TPC can be measured indirectly by knowing the temperature on both sides of the MD membrane and, feed and cold stream temperatures in the bulk. TPC can be calculated using the following Eq. (1);[54]

$$TPC = \left(T_{fm} - T_{pm}\right)/\left(T_f - T_p\right) \quad (1)$$

Where; T_{fm} is the feed side membrane temperature, T_{pm} is the permeate side membrane temperature, T_f is the bulk feed solution temperature and, T_p is the temperature of the bulk coolant/permeate. In an ideal condition, TPC can have a maximum value of 1. A schematic representation of a direct contact membrane distillation (DCMD) experimental setup and the TP profile in a DCMD process are shown in Fig. 6a, b, respectively.

Direct contact membrane distillation (DCMD) experiments

DCMD tests were conducted using a fully automated and programmed MD setup, purchased from Convergence Industry, Netherlands. 1 wt% NaCl solution was used as the feed solution and tap water was used as the coolant. DCMD experiments were conducted at a ΔT of 30 °C, 40 °C, and 50 °C by keeping coolant temperature constant at 15 °C. From past experiences, an optimum flow rate of 60 liters per hour is used on both the feed side and coolant side. All the experiments were carried out for a 24-h time duration. A well-designed membrane module from Convergence with an effective membrane area of 60 cm^2 was used in DCMD experiments. Water permeation flux was calculated using the following Eq. (2);

$$J_w = \Delta w/At \quad (2)$$

Where; 'J_w' is the water permeation flux, 'Δw' is the weight difference of the permeate collected at specific intervals, 'A' is the effective membrane area and 't' is the time. 'J_w' is represented in $Kg/m^2/h$ or $liter/m^2/h$ (LMH). Temperatures of the feed and coolant, at the entrance and exit of the membrane module and, the conductivity of the coolant and feed solutions were automatically measured using respective sensors. An increase in the weight of the coolant tank and a decrease in the weight of the feed tank was monitored periodically and, recorded using a data acquisition system. The coolant tank, feed tank, and tubing were insulated to reduce heat loss. Membrane samples were collected before and after 24-h continuous MD experiments, for performing surface morphology characterizations using FESEM.

DATA AVAILABILITY

The datasets generated during and/or analyzed during the current study are available from the corresponding author on request.

Received: 15 July 2022; Accepted: 9 February 2023;
Published online: 23 February 2023

REFERENCES

1. Schunke, A. J., Hernandez Herrera, G. A., Padhye, L. & Berry, T.-A. Energy recovery in SWRO desalination: current status and new possibilities. *Front. Sustain. Cities.* **2**, 1–7 (2020).
2. Im, B.-G. et al. Comprehensive insights into performance of water gap and air gap membrane distillation modules using hollow fiber membranes. *Desalination* **525**, 115497 (2022).
3. Lee, J.-G. et al. Total water production capacity inversion phenomenon in multi-stage direct contact membrane distillation: A theoretical study. *J. Memb. Sci.* **544**, 126–134 (2017).
4. Ghaffour, N., Missimer, T. M. & Amy, G. L. Technical review and evaluation of the economics of water desalination: current and future challenges for better water supply sustainability. *Desalination* **309**, 197–207 (2013).
5. Maab, H. et al. Synthesis and fabrication of nanostructured hydrophobic polyazole membranes for low-energy water recovery. *J. Memb. Sci.* **423–424**, 11–19 (2012).
6. Nunes, S. P., Maab, H. & Francis, L. Polyazole membrane for water purification. European Patent EP2626127A2 (2022).
7. Amy, G. et al. Membrane-based seawater desalination: present and future prospects. *Desalination* **401**, 16–21 (2017).
8. Mayor, B. Growth patterns in mature desalination technologies and analogies with the energy field. *Desalination* **457**, 75–84 (2019).
9. Tomaszewska, B. et al. Utilization of renewable energy sources in desalination of geothermal water for agriculture. *Desalination* **513**, 115151 (2021).
10. Lotfy, H. R., Staš, J. & Roubík, H. Renewable energy powered membrane desalination — review of recent development. *Environ. Sci. Pollut. Res.* **29**, 46552–46568 (2022).
11. Francis, L., Ahmed, F. E. & Hilal, N. Advances in membrane distillation module configurations. *Membr. (Basel)* **12**, 81 (2022).
12. Macedonio, F. & Drioli, E. Membrane engineering for green process engineering. *Engineering.* **3**, 290–298 (2017).
13. Hammami, M. A. et al. Engineering hydrophobic organosilica nanoparticle-doped nanofibers for enhanced and fouling resistant membrane distillation. *ACS Appl. Mater. Interfaces* **9**, 1737–1745 (2017).
14. Parani, S. & Oluwafemi, O. S. Membrane distillation: recent configurations, membrane surface engineering, and applications. *Membrane* **11**, 934 (2021).
15. Jaworek, A. Electrohydrodynamic microencapsulation technology. In *Encapsulations* 1–45 (Elsevier, 2016). https://doi.org/10.1016/B978-0-12-804307-3.00001-6.
16. Vatanpour, V., Kose-Mutlu, B. & Koyuncu, I. Electrospraying technique in fabrication of separation membranes: a review. *Desalination* **533**, 115765 (2022).
17. Francis, L., Ghaffour, N. & Amy, G. Fabrication and characterization of functionally graded poly(vinylidine fluoride)-silver nanocomposite hollow fibers for sustainable water recovery. *Sci. Adv. Mater.* **6**, 2659–2665 (2014).
18. Contreras-Martínez, J., García-Payo, C. & Khayet, M. Electrospun nanostructured membrane engineering using reverse osmosis recycled modules: membrane distillation application. *Nanomaterials* **11**, 1601 (2021).

19. Bhoje, R., Ghosh, A. K. & Nemade, P. R. Development of performance-enhanced graphene oxide-based nanostructured thin-film composite seawater reverse osmosis. *Membr. ACS Appl Polym. Mater.* **4**, 2149–2159 (2022).
20. Francis, L., Ahmed, F. E. & Hilal, N. Electrospun membranes for membrane distillation: the state of play and recent advances. *Desalination* **526**, 115511 (2022).
21. Francis, L., Ogunbiyi, O., Saththasivam, J., Lawler, J. & Liu, Z. A comprehensive review of forward osmosis and niche applications. *Environ. Sci.* **6**, 1986–2015 (2020).
22. Francis, L. & Hilal, N. Electrosprayed CNTs on electrospun PVDF-Co-HFP membrane for robust membrane distillation. *Nanomaterials* **12**, 4331 (2022).
23. Francis, L. et al. Simultaneous electrospin-electrosprayed biocomposite nanofibrous scaffolds for bone tissue regeneration. *Acta Biomater.* **6**, 4100–4109 (2010).
24. Francis, L. et al. Electrospun polyimide/titanium dioxide composite nanofibrous membrane by electrospinning and electrospraying. *J. Nanosci. Nanotechnol.* **11**, 1154–1159 (2011).
25. Jia, W., Kharraz, J. A., Sun, J. & An, A. K. Hierarchical Janus membrane via a sequential electrospray coating method with wetting and fouling resistance for membrane distillation. *Desalination* **520**, 115313 (2021).
26. Seyed Shahabadi, S. M., Rabiee, H., Seyedi, S. M., Mokhtare, A. & Brant, J. A. Superhydrophobic dual layer functionalized titanium dioxide/polyvinylidene fluoride- co -hexafluoropropylene (TiO_2/PH) nanofibrous membrane for high flux membrane distillation. *J. Memb. Sci.* **537**, 140–150 (2017).
27. Attia, H., Johnson, D. J., Wright, C. J. & Hilal, N. Robust superhydrophobic electrospun membrane fabricated by combination of electrospinning and electrospraying techniques for air gap membrane distillation. *Desalination* **446**, 70–82 (2018).
28. Su, C. et al. Robust superhydrophobic membrane for membrane distillation with excellent scaling resistance. *Environ. Sci. Technol.* **53**, 11801–11809 (2019).
29. Hong, S. K., Kim, H., Lee, H., Lim, G. & Cho, S. J. A pore-size tunable superhydrophobic membrane for high-flux membrane distillation. *J. Memb. Sci.* **641**, 119862 (2022).
30. Aljumaily, M. M. et al. The influence of coating super-hydrophobic carbon nanomaterials on the performance of membrane distillation. *Appl Water Sci.* **12**, 28 (2022).
31. Servi, A. T. et al. A systematic study of the impact of hydrophobicity on the wetting of MD membranes. *J. Memb. Sci.* **520**, 850–859 (2016).
32. Claramunt, S., Völker, F., Gerhards, U., Kraut, M. & Dittmeyer, R. Membranes for the gas/liquid phase separation at elevated temperatures: characterization of the liquid entry pressure. *Membranes* **11**, 907 (2021).
33. Zhang, H., Lamb, R. & Lewis, J. Engineering nanoscale roughness on hydrophobic surface—preliminary assessment of fouling behaviour. *Sci. Technol. Adv. Mater.* **6**, 236–239 (2005).
34. Alhathal Alanezi, A. et al. Theoretical investigation of vapor transport mechanism using tubular membrane distillation module. *Membranes* **11**, 560 (2021).
35. Tomaszewska, M. Temperature polarization coefficient (TPC). In *Encyclopedia of membranes* 1880–1881 (Springer Berlin Heidelberg, 2016). https://doi.org/10.1007/978-3-662-44324-8_574.
36. Zhi, D., Lu, Y., Sathasivam, S., Parkin, I. P. & Zhang, X. Large-scale fabrication of translucent and repairable superhydrophobic spray coatings with remarkable mechanical, chemical durability and UV resistance. *J. Mater. Chem. A Mater.* **5**, 10622–10631 (2017).
37. Borra, J.-P. Review on water electro-sprays and applications of charged drops with focus on the corona-assisted cone-jet mode for High Efficiency Air Filtration by wet electro-scrubbing of aerosols. *J. Aerosol Sci.* **125**, 208–236 (2018).
38. Morais, A. Í. S. et al. Fabrication of polymeric microparticles by electrospray: the impact of experimental parameters. *J. Funct. Biomater.* **11**, 4 (2020).
39. Khayet, M. Membranes and theoretical modeling of membrane distillation: a review. *Adv. Colloid Interface Sci.* **164**, 56–88 (2011).
40. Zhang, H., Liu, M., Sun, D., Li, B. & Li, P. Evaluation of commercial PTFE membranes for desalination of brine water through vacuum membrane distillation. *Chem. Eng. Process. Process Intensif.* **110**, 52–63 (2016).
41. Georgakilas, V., Bourlinos, A. B., Zboril, R. & Trapalis, C. Synthesis, characterization and aspects of superhydrophobic functionalized carbon nanotubes. *Chem. Mater.* **20**, 2884–2886 (2008).
42. Rácz, G. et al. Theoretical and experimental approaches of liquid entry pressure determination in membrane distillation processes. *Periodica Polytechnica Chem. Eng.* **58**, 81–91 (2014).
43. Francis, L., Ghaffour, N., Alsaadi, A. S., Nunes, S. P. & Amy, G. L. Performance evaluation of the DCMD desalination process under bench scale and large scale module operating conditions. *J. Memb. Sci.* **455**, 103–112 (2014).
44. Alsaadi, A. S., Francis, L., Amy, G. L. & Ghaffour, N. Experimental and theoretical analyses of temperature polarization effect in vacuum membrane distillation. *J. Memb. Sci.* **471**, 138–148 (2014).
45. Francis, L., Ghaffour, N., Alsaadi, A. A. & Amy, G. L. Material gap membrane distillation: a new design for water vapor flux enhancement. *J. Memb. Sci.* **448**, 240–247 (2013).
46. Alsaadi, A. S. et al. Modeling of air-gap membrane distillation process: a theoretical and experimental study. *J. Memb. Sci.* **445**, 53–65 (2013).
47. Kim, Y. et al. Osmotically and thermally isolated forward osmosis-membrane distillation (FO-MD) integrated module. *Environ. Sci. Technol.* **53**, 3488–3498 (2019).
48. Alsaadi, A. S., Alpatova, A., Lee, J.-G., Francis, L. & Ghaffour, N. Flashed-feed VMD configuration as a novel method for eliminating temperature polarization effect and enhancing water vapor flux. *J. Memb. Sci.* **563**, 175–182 (2018).
49. Kim, Y.-D., Francis, L., Lee, J.-G., Ham, M.-G. & Ghaffour, N. Effect of non-woven net spacer on a direct contact membrane distillation performance: Experimental and theoretical studies. *J. Memb. Sci.* **564**, 193–203 (2018).
50. Francis, L., Ghaffour, N., Al-Saadi, A. S. & Amy, G. L. Submerged membrane distillation for seawater desalination. *Desalination Water Treat* **55**, 1–6 (2015).
51. Kim, Y.-B., Lee, H.-S., Francis, L. & Kim, Y.-D. Innovative swirling flow-type microbubble generator for multi-stage DCMD desalination system: Focus on the two-phase flow pattern, bubble size distribution, and its effect on MD performance. *J. Memb. Sci.* **588**, 117197 (2019).
52. Korolkov, I. V., Gorin, Y. G., Yeszhanov, A. B., Kozlovskiy, A. L. & Zdorovets, M. V. Preparation of PET track-etched membranes for membrane distillation by photo-induced graft polymerization. *Mater. Chem. Phys.* **205**, 55–63 (2018).
53. Kuang, Z., Long, R., Liu, Z. & Liu, W. Analysis of temperature and concentration polarizations for performance improvement in direct contact membrane distillation. *Int J. Heat. Mass Transf.* **145**, 118724 (2019).
54. Eleiwi, F., Ghaffour, N., Alsaadi, A. S., Francis, L. & Laleg-Kirati, T. M. Dynamic modeling and experimental validation for direct contact membrane distillation (DCMD) process. *Desalination* **384**, 1–11 (2016).

ACKNOWLEDGEMENTS

This work was jointly sponsored by the New York University Abu Dhabi (NYUAD) and Tamkeen under the NYUAD Research Institute Award (Project CG007). All the experiments were conducted using the research facilities at the NYUAD Water Research Center.

AUTHOR CONTRIBUTIONS

L.F.: Conceptualization, Methodology, Experimental, Formal analysis, Data curation, Validation, Characterization, Writing the original draft. N.H.: Funding acquisition, Investigation, Supervision, Writing – review & editing.

COMPETING INTERESTS

The authors declare no competing interests.

ADDITIONAL INFORMATION

Correspondence and requests for materials should be addressed to Nidal Hilal.

Reprints and permission information is available at http://www.nature.com/reprints

Publisher's note Springer Nature remains neutral with regard to jurisdictional claims in published maps and institutional affiliations.